A New Neuronal Cell Protecting Substance, Lavanduquinocin, Produced by *Streptomyces viridochromogenes*

KAZUO SHIN-YA, SHINTARO SHIMIZU, TOSHIHIRO KUNIGAMI, KEIKO FURIHATA, KAZUO FURIHATA† and HARUO SETO*

Institute of Cellular and Molecular Biosciences, University of Tokyo,
†Division of Agriculture and Agricultural Life Sciences, University of Tokyo,
Bunkyo-ku, Tokyo 113, Japan

(Received for publication February 16, 1995)

A new neuronal cell protecting substance, lavanduquinocin was isolated from *Streptomyces viridochromogenes* 2942-SVS3. It consists of a carbazole skeleton with an *ortho* quinone function and a cyclolavandulyl moiety. Lavanduquinocin protected neuronal hybridoma N18-RE-105 cells from L-glutamate toxicity with EC_{50} value 15.5 nM.

It has been well accepted that the excitatory amino acid, L-glutamate acting as a neurotransmitter in the major part of brain, induces neuronal cell death after brain-ischemic attack[1]. L-Glutamate proved to generate oxygen radicals through a variety of intracellular cascades in such events[2]. Under some conditions, brain-ischemia injury is prevented by free radical scavengers[3]. In the course of our screening for substances which protect neuronal hybridoma N18-RE-105 cells from the L-glutamate toxicity, we isolated carquinostatin A[4]. Further investigation has resulted in the isolation of a novel compound named lavanduquinocin (**1**, Fig. 1).

Materials and Methods

Taxonomic Studies

An organism designated 2942-SVS3 was isolated from a soil sample collected in Adachi-ku, Tokyo, Japan. Its characterization and identification were carried out mainly according to BERGEY's Manual[5] and the methods described by SHIRLING and GOTTLIEB[6]. For the evaluation of cultural characteristics, the strain was incubated for 14 days at 27°C. Cell wall composition was analyzed by the methods of BECKER *et al.*[7].

Spectral Analysis

Mass spectra were recorded on a JEOL HX-110 spectrometer in the FAB mode using *m*-nitrobenzyl alcohol as a matrix and polyethylene glycol as internal standard. UV and visible spectra were recorded on a Hitachi U-3210 spectrophotometer and IR spectra were recorded on a Jasco A-102 spectrophotometer. ^1H and ^{13}C NMR spectra were obtained on a JEOL JNM-A500 spectrometer in $(CD_3)_2SO$ solution. Chemical shifts are given in ppm using TMS as internal standard.

Preparation of (*R*)- and (*S*)-MTPA Esters

(*R*)- and (*S*)-MTPA esters of **1** were prepared according to the reported procedures[8]. To a solution of **1** (1.5 mg) in chloroform (1.5 ml) and pyridine (100 μl) was added (+)- or (−)-MTPA chloride (30 mg), and the solution was stirred at room temperature for 3 hours. Methanol (2 ml) was then added, and after stirring for 5 minutes, the solvent was evaporated. The residue was subjected to preparative TLC (Merck, Kieselgel 60, F_{254}, $CHCl_3$-MeOH, 50:1) affording a pure sample of the (*R*)- or (*S*)-MTPA ester of **1**.

Cell and Cell Culture

N18-RE-105 hybrid cells[9] (mouse neuroblastoma clone N18TG-2 × Fisher rat 18-day embryonic neural retina) were grown in a DULBECCO's modified EAGLE's

Fig. 1. Structures of lavanduquinocin (**1**) and carquinostatin A.

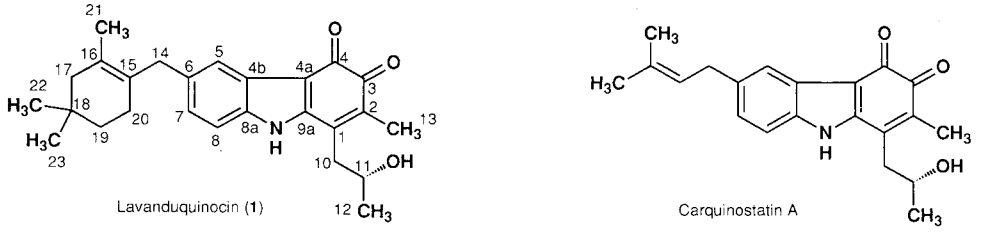

Dedicated to Professor SATOSHI ŌMURA's 60th birthday.

Table 1. Cultural characteristics of strain 2942-SVS3.

	Aerial mycelium	Reverse side color	Soluble pigment
Sucrose-nitrate agar	Not formed	Light orange	None
Glucose-asparagine agar	Green color series	Light orange ~ light reddish orange	None
Glycerol-asparagine agar	Green color series	Light orange	None
Inorganic salts-starch agar	Green color series	Pale yellowish orange	None
Tyrosine agar	Green color series	Reddish brown	Brownish white
Nutrient agar	Not formed	Dull red	None
Yeast-malt agar	Not formed	Pale brown	None
Oatmeal agar	Green color series	Pale reddish orange	None

Fig. 2. Scanning electron micrograph of spore chains of strain 2942-SVS3.

Bar represents 0.5 μm.

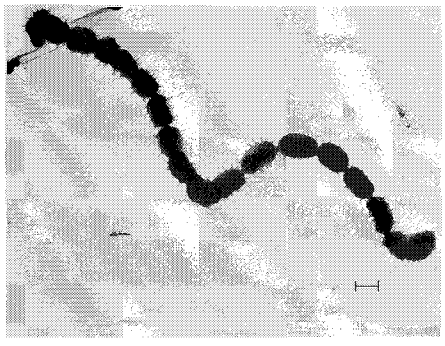

Table 2. Physiological characteristics of strain 2942-SVS3.

Temperature range for growth (°C)	20~45
Production of melanoid pigment	
Tyrosine agar	±
Peptone-yeast-iron agar	+
Tryptone-yeast broth	±
Hydrolysis of starch	+
Liquefaction of gelatin	−
Peptonization of milk	−
Coagulation of milk	−
Reduction of nitrate	+
Utilization of carbon source	
D-Glucose	+
L-Arabinose	+
D-Xylose	+
D-Fructose	+
Sucrose	+
L-Rhamnose	+
Raffinose	+
Inositol	+
D-Mannitol	+

medium supplemented with 0.1 mM hypoxanthine, 0.04 mM aminopterin, 0.14 mM thymidine and 10% heat-inactivated fetal calf serum. The cells were cultured in a humidified atmosphere of 5% CO_2 in air at 37°C. For cytotoxicity studies, cells were plated at 6.25×10^3 cells/cm^2. After culturing for 24 hours, the medium was removed and replaced with a medium containing 10 mM L-glutamate. Cytotoxicity was monitored after 24 hours by a phase-contrast microscope and quantified by the measurement of the cytosolic enzyme, lactate dehydrogenase (LDH), released into the culture medium from degenerated cells[10].

Results

Taxonomy

The substrate mycelium of strain 2942-SVS3 did not fragment. The aerial mycelium irregularly branched on the long main stem and terminated spirals (3~7 rotation), forming spore chains with 10~50 spores per chain. The spores were ellipsoidal (0.45~0.5 × 0.6~0.8 μm) and their surface was spiny (Fig. 2). The culture showed no special morphology such as sporangia, whirls or sclerotia. Whole-cell hydrolysate of strain 2942-SVS3 contained LL-diaminopimelic acid. Accordingly, the cell wall of the strain was classified as type I.

The cultural and physiological properties of strain 2942-SVS3 are summarized in Tables 1 and 2, respectively. Mature aerial mycelia corresponded to the green color series. The reverse side of the colony was light orange to light reddish orange. No soluble pigment except melanoid pigment was observed. The results of these morphological and chemotaxonomic studies indicate that strain 2942-SVS3 belongs to the genus *Streptomyces*. Among the species of *Streptomyces* described in BERGEY's Manual, strain 2942-SVS3 appeared to be most closely related to *Streptomyces viridochromogenes* except the reverse color and soluble pigments. Thus, the strain 2942-SVS3 was identified as *Streptomyces viridochromogenes* 2942-SVS3.

Fermentation

The seed medium consisted of soluble starch 1.0%, molasses 1.0%, meat extract 1.0% and polypepton 1.0% (pH 7.2 before sterilization). Seed tubes containing 15 ml of the medium were inoculated with a stock culture of *S. viridochromogenes* 2942-SVS3 maintained on a BENNET's agar slant, and were incubated on a reciprocal shaker at 27°C for 2 days. The seed culture at 2% was

transferred to 500-ml Erlenmeyer flasks containing 100 ml of a medium consisting of soluble starch 2.5%, soybean meal 1.5%, dried yeast 0.2% and calcium carbonate 0.4% (pH 6.2 before sterilization). The flasks were incubated on a rotary shaker at 27°C for 5 days.

Isolation

The fermentation broth (2 liters) was centrifuged to give a mycelial cake, which was extracted with 500 ml of acetone. The extract was concentrated and the residue was extracted twice with ethyl acetate. The organic fraction was dried over Na_2SO_4, and concentrated to dryness. The oily residue was washed with *n*-hexane, and the residue was applied to a silica gel column (100 ml), which was developed with chloroform - methanol (50 : 1). The active eluate was further purified by HPLC using PEGASIL ODS (Senshu-Pak, 20 i.d. × 250 mm) with 90% methanol. The collected main peak was concentrated to dryness to give a reddish brown powder of **1** (4 mg).

Physico-chemical Properties

The physico-chemical properties of **1** are summarized in Table 3. The molecular formula of **1** was established as $C_{26}H_{31}NO_3$ by high-resolution FAB-MS. UV and visible spectra revealed the presence of a chromophore in **1** identical or similar to that in carquinostatin A[4] (Fig. 1). IR absorptions at 1645 and 1620 cm^{-1} implied the presence of a quinone carbonyl function.

Structure Elucidation

The ^1H NMR spectrum and tabulated ^{13}C NMR spectral data are shown in Fig. 3 and Table 4, respectively.

The phase-sensitive DQF spectrum revealed the presence of a 1,2,4-trisubstituted benzene ring. A

Table 3. Physico-chemical properties of lavanduquinocin (**1**).

Appearance	Reddish brown powder
MP	157~158°C
Molecular formula	$C_{26}H_{31}NO_3$
HRFAB-MS (*m/z*)	
Found	406.2394 $(M+H)^+$
Calcd	406.2382
UV λ_{max}^{MeOH} nm (ε)	232 (17,500), 269 (15,900), 429 (3,100)
$\lambda_{max}^{MeOH+NaOH}$ nm (ε)	244 (16,400), 288 (16,300), 472 (4,300)
IR ν_{max} (KBr) cm^{-1}	3450, 3220, 1660 (sh), 1640 (sh), 1615

Table 4. ^{13}C and ^1H chemical shifts of lavanduquinocin (**1**) in DMSO-d_6.

No.	δ_C	δ_H	No.	δ_C	δ_H
1	140.1		11	65.9	3.95
2	134.3		12	23.7	1.23
3	183.9		13	12.1	1.91
4	172.5		14	38.4	3.41
4a	110.7		15	127.3	
4b	126.2		16	125.6	
5	119.4	7.63	17	45.6	1.78
6	136.7		18	28.9	
7	124.5	6.98	19	35.4	1.24
8	113.4	7.40	20	26.8	1.84
8a	136.0		21	19.6	1.73
9a	146.7		22, 23	28.1	0.84
10	37.7	2.74			

Fig. 3. ^1H NMR spectrum of **1** in DMSO-d_6.

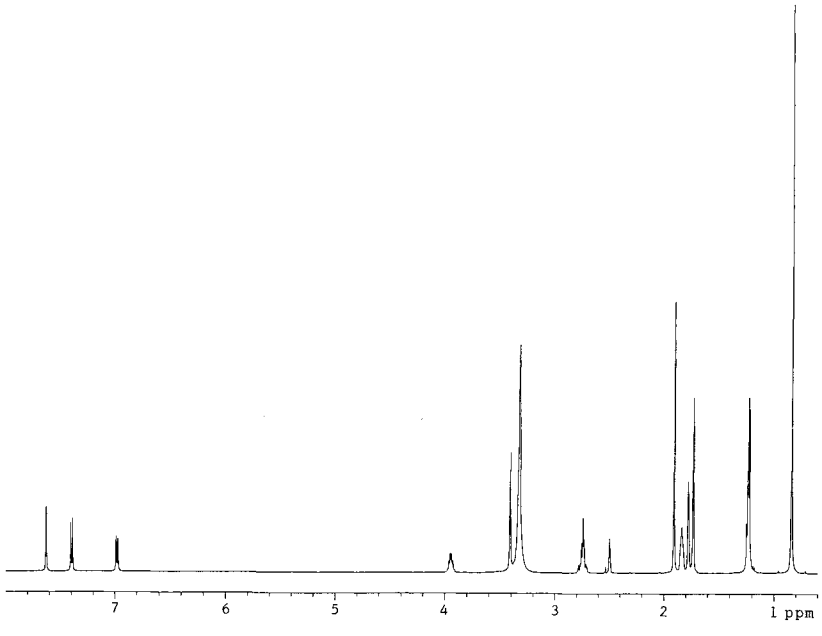

Fig. 4. Partial structures of **1**.

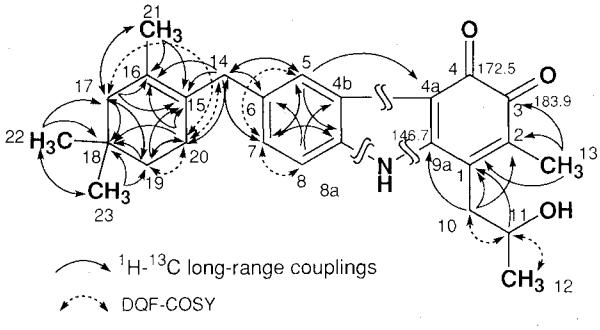

Fig. 5. Preventive effect of lavanduquinocin and carquinostatin A on glutamate toxicity in N18-RE-105 cells.

○ lavanduquinocin, ● carquinostatin A.

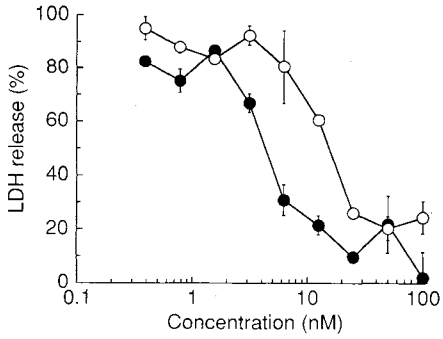

methylene proton signal 19-H (1.24 ppm) was coupled to a methylene proton signal 20-H (1.84 ppm) which showed long-range couplings with methylene protons 17-H (1.78 ppm) and 14-H (3.41 ppm). Singlet methyl protons 22, 23-H (0.84 ppm, 6H) showed ^{1}H-^{13}C long-range couplings to C-17 (45.6 ppm), C-18 (28.9 ppm) and C-19 (35.4 ppm) in the HMBC spectrum. In addition, an allylic methyl proton 21-H (1.73 ppm) was coupled to C-15 (127.3 ppm), C-16 (125.6 ppm) and C-17 (45.6 ppm). The connectivity between C-14 (38.4 ppm) and C-15 was also confirmed by the long-range couplings from 14-H to C-15, C-16 and C-20 (26.8 ppm). These results indicated the presence of a cyclolavandulyl moiety[11] (Fig. 4). Aromatic protons 5-H (7.63 ppm) and 7-H (6.98 ppm) showed the long-range couplings to C-14. Thus, the cyclolavandulyl moiety was linked to the C-6 (136.7 ppm) position of the 1,2,4-trisubstituted benzene ring explained above. Other ^{1}H-^{13}C long-range couplings revealed by the HMBC experiments are shown in Fig. 4.

Another substructure was determined as follows. The sequence from methylene protons 10-H (2.74 ppm) to methyl protons 12-H (1.23 ppm) through an oxymethine proton 11-H (3.95 ppm) revealed the presence of a 2-hydroxypropyl residue. The terminal methylene signal of this unit (10-H) was long-range coupled to aromatic carbons C-1 (140.1 ppm), C-2 (134.3 ppm) and C-9a (146.7 ppm). An aromatic methyl proton resonance 13-H (1.91 ppm) was coupled to aromatic carbons C-1, C-2 and a quinone carbonyl carbon C-3 (183.9 ppm). Since the ^{13}C chemical shift of C-9a (146.7 ppm), which was *para* to a carbonyl carbon C-3, was too high to be assigned to a quinone carbonyl carbon, the quinone system was concluded to be an *ortho* system; this function being supported by the UV and visible spectra of **1**. Thus, the other quinone carbonyl carbon C-4 (172.5 ppm) and the remaining aromatic carbon C-4a (110.7 ppm) were assigned as shown in Fig. 4. The linkage between these two substructures was established by long-range coupling of 5-H to C-4a, and by comparison of the ^{13}C chemical shifts of **1** with those of carquinostatin A.

The absolute stereochemistry at C-11 position of **1** was determined to be *R* by the modified MOSHER method[8,12]. Thus, 10-H and 13-H resonated at upper field in the (*S*)-ester than in the (*R*)-ester ($\Delta\delta$, -0.05 ppm and -0.03 ppm, respectively. $\Delta\delta=\delta_S-\delta_R$). Moreover, 12-H appeared upfield for the (*R*)-ester than for the (*S*)-ester ($\Delta\delta$, $+0.02$ ppm). Structurally **1** with a carbazole skeleton incorporating an *ortho* quinone function is related to carquinostatin A and carbazoquinocins[13].

Biological Activity

In the evaluation system we employed[14,15], **1** and carquinostatin A decreased the L-glutamate toxicity to N18-RE-105 cells with EC_{50} values 15.5 nM and 4.3 nM, respectively (Fig. 5). Apoptotic cell death of N18-RE-105 cells induced by buthionine sulfoximine (BSO) as a result of depletion of glutathione, an endogenous reducing agent[16], was also suppressed by **1** at concentrations higher than 12.5 nM. This toxicity of BSO is considered to involve oxygen radicals.

Discussion

Lavanduquinocin showed a strong activity to suppress the L-glutamate toxicity in neuronal hybridoma N18-RE-105 cells. It consists of a carbazole nucleus with an *ortho* quinone function and a cyclolavandulyl moiety, and structurally related to carquinostatin A, a metabolite of *Streptomyces exfoliatus*. It is interesting to note that they possess at the same position a monoterpenoidal side chain, which is rarely found in the metabolites of *Streptomyces*.

The L-glutamate toxicity to N18-RE-105 cells is calcium dependent[17] and mainly caused by inhibition of cystine uptake[15]. This toxicity is blocked by mem-

brane depolarization caused by, for example, ouabain or treatment of high concentrations of KCl[18], and is blocked by reducing agents such as dithiothreitol and glutathione[14]. Since lavanduquinocin suppressed the BSO toxicity, it presumably acts as a reducing agent instead of glutathione in N18-RE-105 cells. Thus the mode of action of lavanduquinocin is thought to be mainly dependent on its antioxidative activity. Further investigation on its biological activity is now under way.

Acknowledgments

This work was supported in part by a Grant-in Aid for Encouragement of Young Scientists, The Ministry of Education, Science and Culture, Japan to K. S.

References

1) Choi, D. W.: Cerebral hypoxia: some approaches and unanswered questions. J. Neurosci. 10: 2493~2501, 1990
2) Coyle, J. T. & P. Puttfarcken: Oxidative stress, glutamate, and neurodegenerative disorders. Science 262: 689~695, 1993
3) Kinouchi, H.; C. J. Epstein, T. Mizui, E. Carlson, S. F. Chen & P. H. Chan: Attenuation of focal cerebral ischemic injury in transgenic mice overexpressing CuZn superoxide dismutase. Proc. Natl. Acad. Sci. U.S.A. 88: 11158~11162, 1991
4) Shin-ya, K.; M. Tanaka, K. Furihata, Y. Hayakawa & H. Seto: Structure of carquinostain A, a new neuronal cell protecting substance produced by *Streptomyces exfoliatus*. Tetrahedron Lett. 34: 4943~4944, 1993
5) Locci, R.: Streptomyces and related genera. *In* Bergey's Manual of Systematic Bacteriology. Vol. 4. *Ed.*, S. T. Williams *et al.*, pp. 2451~2508, Williams & Wilkins, 1989
6) Shirling, E. B. & D. Gottlieb: Methods for characterization of *Streptomyces* species. Int. J. Syst. Bacteriol. 16: 313~340, 1966
7) Becker, B.; M. P. Lechvalier & H. A. Lechevalier: Chemical composition of cell wall preparations from strains of various genera of aerobic actinomycetes. Appl. Microbiol. 13: 236~243, 1965
8) Dale, J. A. & H. S. Mosher: Nuclear magnetic resonance enantiomer reagents. Configurational correlations *via* nuclear magnetic resonance chemical shifts of diastereomeric mandelate, *O*-methylmandelate, and α-methoxy-α-trifluoromethylphenylacetate (MTPA) esters. J. Am. Chem. Soc. 95: 512~519, 1973
9) Malouf, A. T.; R. L. Schnaar & J. T. Coyle: Characterization of glutamic acid neurotransmitter binding site on neuroblastoma hybrid cells. J. Biol. Chem. 20: 12756~12762, 1984
10) Koh, J. & D. W. Choi: Vulnerability of cultured cortical neurons to damage by excitotoxins: differential susceptibility of neurons containing NADPH-diaphorase. J. Neurosci. 8: 2153~2163, 1988
11) Imai, S.; K. Furihata, Y. Hayakawa, T. Noguchi & H. Seto: Lavanducyanin, a new antitumor substance produced by *Streptomyces* sp. J. Antibiotics 42: 1196~1198, 1989
12) Ohtani, I.; T. Kusumi, Y. Kashman & H. Kakisawa: High-field FT NMR application of Mosher's method. The absolute configurations of marine terpenoids. J. Am. Chem. Soc. 113: 4092~4096, 1991
13) Tanaka, M.; K. Shin-ya, K. Furihata & H. Seto: Isolation and structural elucidation of antioxidative substances, carbazoquinocins A to F. J. Antibiotics 48: 326~328, 1995
14) Miyamoto, M.; T. H. Murphy, R. L. Schnaar & J. T. Coyle: Antioxidants protect against glutamate-induced cytotoxicity in a neuronal cell line. J. Pharmacol. Exp. Ther. 250: 1132~1140, 1989
15) Murphy, T. H.; M. Miyamoto, A. Sastre, R. L. Schnaar & J. T. Coyle: Glutamate toxicity in a neuronal cell line involves inhibition of cystine transport leading to oxidative stress. Neuron 2: 1547~1558, 1989
16) Kane, D. J.; T. A. Sarafian, R. Anton, H. Hahn, E. B. Gralla, J. S. Valentine, T. Örd & D. E. Bredesen: Bcl-2 inhibition of neural death: Decreased generation of reactive oxygen species. Science 262: 1274~1277, 1993
17) Murphy, T. H.; A. T. Malouf, A. Sastre, R. L. Schnaar & J. T. Coyle: Calcium-dependent glutamate cytotoxicity in a neuronal cell line. Brain Res. 444: 325~332, 1988
18) Murphy, T. H.; R. L. Schnaar, J. T. Coyle & A. Sastre: Glutamate cytotoxicity in a neuronal cell line is blocked by membrane depolarization. Brain Res. 460: 155~160, 1988